Neural Process Lett (2018) 47:509–533
https://doi.org/10.1007/s11063-017-9664-9

Finite-Time Robust Synchronization of Memrisive Neural Network with Perturbation

Hui Zhao[1,2] · Lixiang Li[4,5] · Haipeng Peng[4,5] · Jürgen Kurths[6] · Jinghua Xiao[2] · Yixian Yang[3,4,5]

Published online: 15 July 2017

Abstract In this paper, we study finite-time synchronization of a memristive neural network (MNN) with impulsive effect and stochastic perturbation. Because the parameters of the MNN are state-dependent, the traditional analytical method and control technique can not be directly used. In previous research, differential inclusions theory and set-valued mappings technique have been recently introduced to deal with this MNN system. But, we study the synchronization of MNN without using the previous solution technique. A novel analytical technique is first proposed to transform the MNN to a class of neural network (cNN) with uncertain parameters. The finite-time synchronization is obtained by disposing of parameter mismatch, impulsive effect or stochastic perturbation for the cNN. Several useful criteria of synchronization are obtained based on Lyapunov function, linear matrix inequality (LMI) and finite-time stability theory. Finally, two examples are given to demonstrate the effectiveness of our proposed method.

Keywords Finite-time synchronization · Memristive neural network · Impulsive effect · Stochastic perturbation

✉ Lixiang Li
li_lixiang2006@163.com

Hui Zhao
hz_paper@163.com

1 Shandong Provincial Key Laboratory of Network Based Intelligent Computing, School of Information Science and Engineering, University of Jinan, Jinan 250022, China

2 State Key Laboratory of Information Photonics and Optical Communications, School of Science, Beijing University of Posts and Telecommunications, Beijing 100876, China

3 State Key Laboratory of Public Big Data, Guizhou 550025, China

4 State Key Laboratory of Networking and Switching Technology, Information Security Center, Beijing University of Posts and Telecommunications, P.O. Box 145, Beijing 100876, China

5 The National Engineering Laboratory for Disaster Backup and Recovery, Beijing University of Posts and Telecommunications, Beijing 100876, China

6 Potsdam Institute for Climate Impact Research, 14473 Potsdam, Germany

1 Introduction

Memristor was first proposed by Leon Chua in 1971 [1], who reasoned from physical symmetry arguments that, besides the resistor, capacitor and inductor, there should be a fourth circuit element which he called memristor. Unlike the other three fundamental circuit elements, the memristor is a nonlinear one and its value is not unique, it describes the relationship between electric charge and magnetic flux, as shown in Fig. 1.

The memristor's current-voltage characteristics are caused by its nonlinearity and external periodic voltage. The memristor can memorize its history, which means that when the voltage is turned off, the memristor remembers its most recent value until next time it is turned on. The memory characteristic was determined by its physical structure and external input. Memristor is a switchable device. A thin film between two metals separates the passive device into two regions: the doped and the undoped ones, which is shown in Fig. 2.

In 2013, Thomas used memristive systems to mimic the synaptic functionality of the brain with a simple device [2]. He explain that they can utilize memristors to pave the way to computer architectures that are more similar to the (human) brain than von-Neumann computers. In principle, neural networks work as a combination of neurons and synapses. Electronic devices can easily emulate the neurons and their behavior, however, it turned out to be more difficult to mimic the synaptic functionality. The memristor can fill this gap and also allows the access to analog values. Memristor is able to continuously increase or reduce resistance just as the process of learning and forgetting in the human brain. Therefore, the memristor was considered to be the electronic equivalent of the synapse, which is shown in Fig. 3.

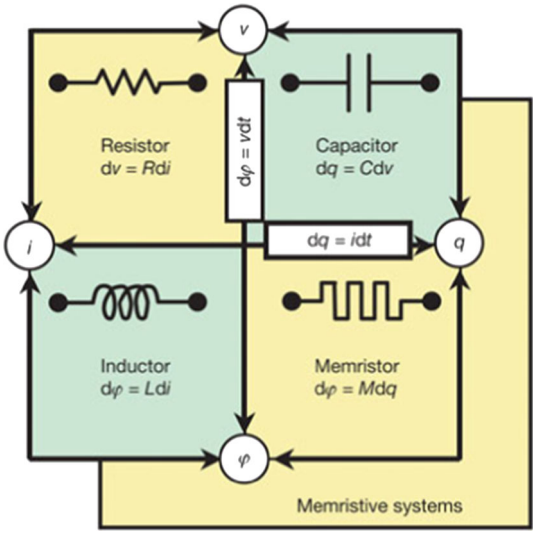

Fig. 1 The physical symmetry relations between the four fundamental circuit elements

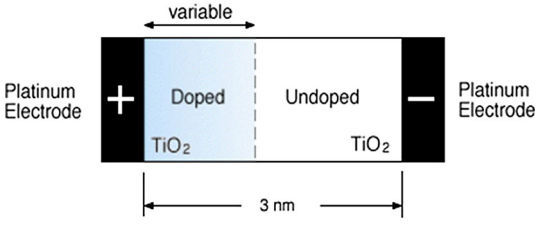

Fig. 2 A switchable device shows the principle of TiO_2 memristor

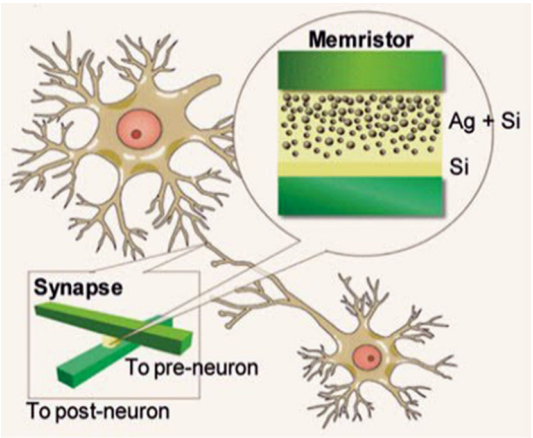

Fig. 3 The electronic equivalent of the synapse: memristor

As the memristor is well used to mimic a synapse, we can substitute the memristor for synapse in the artificial neural network. Therefore, the model of MNN which is widely applied in the associative memory, the next generation computer and powerful brain-like "neural" computer, is a more realistic model for the description of real neural systems. Recently, many interesting results have been obtained on MNN stability and synchronization [3–5]. It is well known that the parameters of MNN are state dependent, the traditional robust analytical technique can not be directly used [6]. Therefore, existing results on stability and synchronization use the differential inclusions theory and set-valued mappings technique to deal with differential equations with a MNN system. Different kinds of synchronization were investigated for the MNN including anti-synchronization [7], projective synchronization [8, 9], stochastic synchronization [10,11] and others [12–15]. Many control techniques including adaptive control [15], impulsive control [16,17], intermittent control [18] etc. have been widely investigated for the MNN.

In the process of the drive-response system achieving synchronization, the state-parameters of drive-response MNN may be mismatched before the synchronization is realized due to the fact that parameters of MNN are state-dependent. Hence, it is difficult to study the dynamic behaviour of MNN via the classical analytical techniques. Although there are many results on robust synchronization of neural network with bounded uncertain parameters, the bounded uncertain parameters of the drive-response in the neural networks are restricted to being identical. Hence the traditional robust analytical techniques for robust performance analysis of neural networks with matched uncertain parameters can not be directly utilized to study synchronization of MNN. In the paper, our aim is to develop a novel analytical techniques to transform MNN into cNN with uncertain parameters to study synchronization performance. In previous research, the finite-time boundedness was investigated for the MNN based on this transformation technique [19], in which the MNN without time-delays and with time-varying delays are fully considered.

In the applications, there exist typically some uncertain parameters and noise perturbations in real systems [20,21], including impulsive effect and stochastic perturbation, which often affect the dynamics of nonlinear systems. In a real neural system, there is usually affected by external perturbations and such perturbations may be treated as fluctuations from the release of neurotransmitters and other probabilistic causes. The existence of random uncertainties including the internal or external noises, these stochastic noise in the electrical circuits design of neural networks possesses an important source, which may be the key

factors to lead to system instability. Besides, it could trigger financial crisis in the financial system and cause blackouts and huge economic losses. Therefore, the noise perturbation must be taken into consideration for complex networks, which cannot be ignored. For a general nonlinear dynamical networks, Lu et al. [22,23] consider pinning impulsive stabilization issue and outer synchronization behavior in pinning impulsive controllers. So it has important practical implication to investigate synchronization issues of uncertain complex dynamical systems based on robust control techniques. Besides, taking secure communication for example, compared with asymptotic synchronization and exponential synchronization, finite-time synchronization is here considered based on the finite-time stability theory [24]. This enables us to recover the transmitted signals in a setting time, which improve the efficiency and the confidentiality greatly. For neural systems and neural networks, there is a certain time delay between the spread of neurotransmitter and time-delay is time-varying in most real situations [25,26]. To our best knowledge, few works have been done on the finite-time synchronization for MNN with impusive disturbance and stochastic perturbation based on this transformation. Therefore, it is of great value both practically and theoretically to study FTB of MNN with the time-varying delay.

Motivated by the above analysis, we consider finite-time synchronization for the MNN with impulsive effect and stochastic perturbation in this paper. Different from previous techniques in dealing with the MNN system, we use a novel technique that transforms the MNN into cNN to study its dynamical behaviour. To achieve the finite-time synchronization, those difficult about parameter mismatch is overcame and those perturbation about impulsive effect and stochastic perturbation are, respectively, considered based on stochastic differential equations and finite-time stability theory. Several sufficient conditions are obtained and an appropriate controller is designed to guarantee finite-time synchronization of MNN both with impulsive effect and stochastic perturbation.

This paper is organized as follows. In Sect. 2, the network model and preliminaries are given. In Sect. 3, main results about finite-time synchronization of MNN with both impulsive effect and stochastic perturbation are obtained by constructing an appropriate Lyapunov function and designing an appropriate controller. In Sect. 4, numerical examples are given to demonstrate the effectiveness of proposed methods. Finally, conclusions and prospects are given in Sect. 5.

Notations: Throughout this paper, if not explicitly stated, matrices are assumed to have compatible dimensions. R denotes the set of real numbers, R^n and $R^{m\times n}$ refer to, respectively, the n dimensional Euclidean space and the set of all $m \times n$ real matrices. $\|x\| = (\sum_{i=1}^{n} x_i^2)^{\frac{1}{2}}$. The notation $P > 0$ means P is real symmetry positive definite and the superscript T stands for the transpose for vector or matrices. In addition, $*$ refers to the ellipsis in symmetric matrices expressions and I denotes the identity matrix with the appropriate dimension.

2 Problem Formulation and Preliminaries

We consider the following MNN as drive system, which is given as

$$\begin{aligned}\dot{x}_i(t) = &-c_i x_i(t) + \sum_{j=1}^{n} a_{ij}(x_i(t))\bar{g}_j(x_j(t)) \\ &+ \sum_{j=1}^{n} b_{ij}(x_i(t))g_j(x_j(t-\tau(t))) + I_i, \\ &t \geq 0, i = 1, 2, \ldots, N, \end{aligned} \tag{1}$$

where

$$c_i = \frac{1}{C_i}\left[\sum_{j=1}^{n}(W_{\bar{g}ij} + W_{gij}) \times sgn_{ij} + \frac{1}{R_i}\right],$$

$$a_{ij}(x_i(t)) = \frac{W_{\bar{g}ij}}{C_i} \times sgn_{ij}, \quad b_{ij}(x_i(t)) = \frac{W_{gij}}{C_i} \times sgn_{ij},$$

$x_i(t) = (x_1(t), x_2(t), \ldots, x_n(t))$ is the state scalar of the ith neuron at time t, I_i is the external input to the ith neuron. $\tau(t)$ is the time-varying delay satisfying $0 \le \tau(t) \le \tau$ and $\dot{\tau}(t) \le \mu < 1$, where τ and μ are given constants; $\bar{g}_j(x_j(t))$ and $g_j(x_j(t-\tau(t)))$ are, respectively, the bounded feedback functions without and with time-varying time delay between the memristor and $x(t)$; c_i is the ith neuron self-inhibitions, $a_{ij}(x_i(t))$ and $b_{ij}(x_i(t))$ represent the non-delayed and delayed memristive synaptic weights, respectively.

Remark 1 For the model of MNN, compared with the electric circuits in Zhao, Li, & Peng, 2015 etc., the memductances of the memristors $W_{\bar{g}ij}$, W_{gij} and R_i, respectively take place of the resistors R_{ij}, F_{ij} and R_i of a general class of neural networks. MNN can be implemented by very large-scale integration (VLSI) circuits as shown in Fig. 1.

We suppose that the above state-dependent parameters satisfy the following conditions:

$$a_{ij}(x_i(t)) = \begin{cases} \hat{a}_{ij}, & |x_i| \le T_i, \\ \check{a}_{ij}, & |x_i| > T_i, \end{cases} \tag{2}$$

$$b_{ij}(x_i(t)) = \begin{cases} \hat{b}_{ij}, & |x_i| \le T_i, \\ \check{b}_{ij}, & |x_i| > T_i, \end{cases} \tag{3}$$

where the switching jumps $T_i > 0$, $\hat{a}_{ij}$, $\check{a}_{ij}$, $\hat{b}_{ij}$, $\check{b}_{ij}$, $i, j = 1, 2, \ldots, N$, are all constants (Fig. 4).

Remark 2 The memristor's current-voltage characteristics are caused by its nonlinearity and external periodic voltage. The memristor can memorize its history, i.e., when the voltage is turned off, the memristor remembers its most recent value until next time it is turned on. The pinched hysteresis loop is due to the nonlinear relationship between the memristance current and voltage which is shown in Fig. 2. The memristor exhibits the feature of pinched hysteresis, i.e., that a lag occurs between the application and the removal of a field and its subsequent effect, just as neurons in the human brain do.

In the next analysis, a novel technique is proposed to transform a MNN system to a cNN with uncertain parameters, and the finite-time synchronization is obtained by investigating this cNN. Denote $\bar{a}_{ij} = \max\{\hat{a}_{ij}, \check{a}_{ij}\}$, $\underline{a}_{ij} = \min\{\hat{a}_{ij}, \check{a}_{ij}\}$, $\bar{b}_{ij} = \max\{\hat{b}_{ij}, \check{b}_{ij}\}$, $\underline{b}_{ij} = \min\{\hat{b}_{ij}, \check{b}_{ij}\}$, $a_{ij} = \frac{1}{2}(\bar{a}_{ij} + \underline{a}_{ij})$, $\tilde{a}_{ij} = \frac{1}{2}(\bar{a}_{ij} - \underline{a}_{ij})$, $b_{ij} = \frac{1}{2}(\bar{b}_{ij} + \underline{b}_{ij})$, $\tilde{b}_{ij} = \frac{1}{2}(\bar{b}_{ij} - \underline{b}_{ij})$ (Fig. 5).

Therefore, the MNN (1) is a special case of a cNN and it can be written as:

$$\begin{aligned} \dot{x}_i(t) = &-c_i x_i(t) + \sum_{j=1}^{n}(a_{ij} + \triangle a_{1ij})\bar{g}_j(x_j(t)) \\ &+ \sum_{j=1}^{n}(b_{ij} + \triangle b_{1ij})g_j(x_j(t-\tau(t))) + I_i, \\ &t \ge 0, i = 1, 2, \ldots, N, \end{aligned} \tag{4}$$

where $x_i(t) = \varphi_i(t) \in C([-\tau, 0], R)$, $\triangle a_{1ij} \in [-\tilde{a}_{ij}, \tilde{a}_{ij}]$, $\triangle b_{1ij} \in [-\tilde{b}_{ij}, \tilde{b}_{ij}]$.

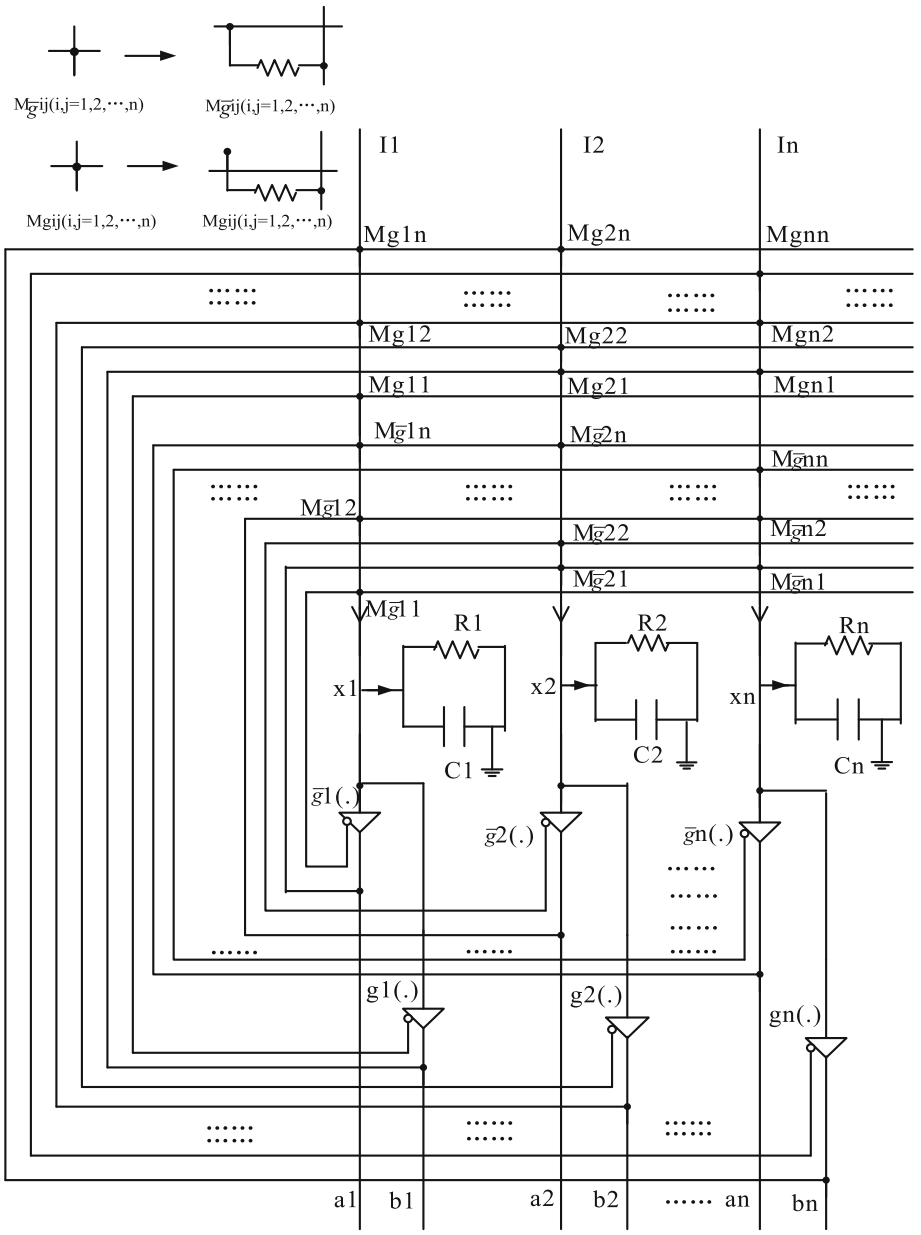

Fig. 4 Circuit of MNN, where $x_i(\cdot)$ is the state of the ith subsystem, $\bar{f}_j(\cdot)$, $g_j(\cdot)$ are the amplifiers, $W_{\bar{g}ij}(\cdot)$ is the connection memristor between the amplifier $\bar{g}_j(\cdot)$ and state $x_i(\cdot)$ and $W_{gij}(\cdot)$ is the connection memristor between the amplifier $g_j(\cdot)$ and state $x_i(\cdot)$, R_i and C_i are the resistor and capacitor, I_i is the external input, a_i, b_i are the outputs

Remark 3 It is well known that under the conditions of state-dependence, the variables $\triangle a_{1ij}$ and $\triangle b_{1ij}$ may not reach their maximum and minimum values at the same time. Therefore, we set $\triangle a_{1ij} = F_1(t)\tilde{a}_{ij}$ and $\triangle b_{1ij} = F_2(t)\tilde{b}_{ij}$, where $F_1(t), F_2(t) \in [-1, 1]$.

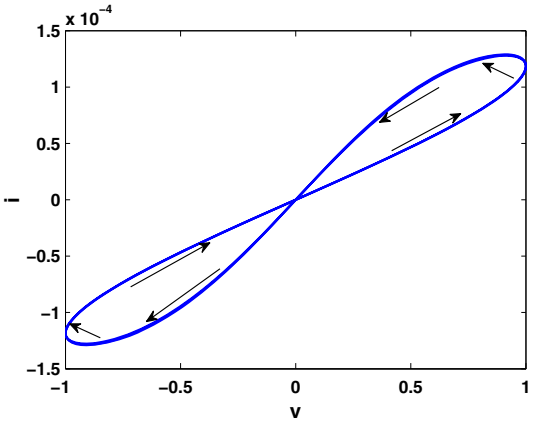

Fig. 5 Typical current-voltage (i-v) characteristics of a memristor

In particular, when $\hat{a}_{ij} > \check{a}_{ij}$ and $\hat{b}_{ij} > \check{b}_{ij}$ or $\hat{a}_{ij} < \check{a}_{ij}$ and $\hat{b}_{ij} < \check{b}_{ij}$, the variables $\triangle a_{1ij}$, and $\triangle b_{1ij}$ can reach their maximum and minimum values at the same time. In this case, $F_1(t) = F_2(t) = F(t) \in [-1, 1]$.

The corresponding response system can be rewritten in the following form of an impulsive differential equation:

$$\begin{aligned}\dot{y}_i(t) = &-c_i y_i(t) + \sum_{j=1}^{n} a_{ij}(y_i(t))\bar{g}_j(y_j(t)) \\ &+ \sum_{j=1}^{n} b_{ij}(y_i(t))g_j(y_j(t-\tau(t))) + I_i, \\ &+ u_i(t),\ i = 1, 2, \ldots, N,\ t \neq t_k, \end{aligned} \tag{5}$$

and

$$\begin{aligned}&\triangle y_i(t) = y_i(t_k^+) - y_i(t_k^-) = B_{ik}e_i(t_k),\ t = t_k,\ k \in \ell, \\ &y_i(t_0^+) = y_i(0),\end{aligned}$$

where $y_i = (y_1, y_2, \ldots, y_n)^T$ is the response state scalar of the ith node. $a_{ij}(y_i(t))$ and $b_{ij}(y_i(t))$ are, respectively, defined similar with (2) and (3). $u_i(t)$ is a controller to be designed. The initial conditions of (5) are defined by $y_i(t) = \psi_i(t) \in C([-\tau, 0], R), i = 1, 2, \ldots, n$, $y_i(t_k^+) = \lim_{t \to t^+} y_i(t)$, $y_i(t_k^-) = \lim_{t \to t^-} y_i(t)$. $\ell = \{1, 2, \ldots, n, n_1, \ldots, n_k\}$ is a finite natural number set. For simplicity, it is assumed that $y_i(t_k^-) = y_i(t_k)$, which means $y_i(t)$ is left continuous at each t_k. The moments of impulse satisfy $t_1 < t_2 < \ldots < t_k < t_{k+1} < \ldots$ and $\lim_{k \to \infty} t_k = \infty, e_i(t_k) = y_i(t_k) - x_i(t_k)$ and $\tau_k = t_k - t_{k-1} < \infty$. $u_i(t) (i = 1, 2, \ldots, N)$ is a nonlinear controller to be designed.

Similar to (1), the MNN (5) is also a special case of cNN as follows:

$$\begin{aligned}\dot{y}_i(t) = &-c_i y_i(t) + \sum_{j=1}^{n} (a_{ij} + \triangle a_{2ij})\bar{g}_j(y_j(t)) \\ &+ \sum_{j=1}^{n} (b_{ij} + \triangle b_{2ij})g_j(y_j(t-\tau(t))) + I_i \\ &+ u_i(t),\ t \neq t_k, i = 1, 2, \ldots, N, \end{aligned} \tag{6}$$

and

$$\triangle y_i(t) = y_i(t_k^+) - y_i(t_k^-) = B_{ik}e_i(t_k),\ t = t_k,\ k \in \ell,$$

where $\triangle a_{2ij} \in [-\tilde{a}_{ij}, \tilde{a}_{ij}]$ and $\triangle b_{2ij} \in [-\tilde{b}_{ij}, \tilde{b}_{ij}]$.

Remark 4 Obviously, the variables $\triangle a_{2ij}$ and $\triangle b_{2ij}$ may not reach their maximum and minimum values at the same time. We set $\triangle a_{2ij} = E_1(t)\tilde{a}_{ij}$ and $\triangle b_{2ij} = E_2(t)\tilde{b}_{ij}$, where $E_1(t), E_2(t) \in [-1, 1]$. Since the initial conditions of (4) and (6) are different, $\triangle a_{1ij}$ and $\triangle b_{1ij}$ may not be equal to $\triangle a_{2ij}$ and $\triangle b_{2ij}$, where $F_i(t), i = 1, 2$ may be different from $E_i(t), i = 1, 2$. These problems of parameter mismatch imply that the traditional robust technique can not be directly used to achieve finite-time synchronization of a cNN with uncertain parameters.

Denote $A = (a_{ij})_{n\times n}$, $B = (b_{ij})_{n\times n}$, $\tilde{A} = (\tilde{a}_{ij})_{n\times n}$, $\tilde{B} = (\tilde{b}_{ij})_{n\times n}$ and $I = (I_1, I_2, \ldots, I_n)$, the system (4) can be written as

$$\begin{aligned}\dot{x}(t) = &-Cx(t) + (A + \triangle A_1(t))\bar{g}(x(t)) \\ &+ (B + \triangle B_1(t))g(x(t - \tau(t))) + I,\end{aligned} \tag{7}$$

where $x(t) = (x_1(t), x_2(t), \ldots, x_N(t))$, according to Assumption 1, $[\triangle A_1(t), \triangle B_1(t)] = [F_1(t)\tilde{A}, F_2(t)\tilde{B},] = [H_1F_1(t)M_1, H_2F_2(t)M_2]$, $F_i(t) \in [-1, 1], i = 1, 2$.

The system (6) with impulsive effect and control input is given as

$$\begin{aligned}\dot{y}(t) = &-Cy(t) + (A + \triangle A_2(t))\bar{g}(y(t)) \\ &+ (B + \triangle B_2(t))g(y(t - \tau(t))) + I + u(t),\ t \neq t_k, \\ \triangle y(t) = &\ y(t_k^+) - y(t_k^-) = B_k e(t_k),\ t = t_k,\ k \in \ell,\end{aligned} \tag{8}$$

where $y(t) = (y_1(t), y_2(t), \ldots, y_n(t))$, according to Assumption 1, $\triangle A_2(t)$, $\triangle B_2(t)$ are also be obtained.

Let $e(t) = y(t) - x(t)$ be the synchronization error. Then we yield the error system from systems (7) and (8) as follows:

$$\begin{aligned}\dot{e}(t) = &-Ce(t) + (A + \triangle A_2(t))f(e(t)) \\ &+ (B + \triangle B_2(t))f(e(t - \tau(t))) \\ &+ (\triangle A_2(t) - \triangle A_1(t))g(x(t)) \\ &+ (\triangle B_2(t) - \triangle B_1(t))g(x(t - \tau(t))) \\ &+ u(t),\ t \neq t_k, \\ e(t_k^+) = &\ y(t_k^+) - x(t_k^+) = y(t_k) - x(t_k) + B_k e(t_k), \\ = &\ (I + B_k)e(t_k),\ t = t_k,\ k \in \ell,\end{aligned}$$

where $f(e(\cdot)) = \bar{g}(e(\cdot) + x(\cdot)) - \bar{g}(x(\cdot)) = g(e(\cdot) + x(\cdot)) - g(x(\cdot))$.

System (7) can be written as

$$\begin{aligned}dx(t) = &[-Cx(t) + (A + \triangle A_1(t))\bar{g}(x(t)) \\ &+ (B + \triangle B_1(t))g(x(t - \tau(t))) + I]\,dt.\end{aligned} \tag{9}$$

The MNN is converted to a cNN with stochastic perturbation, which can be written as the following stochastic differential equation

$$\begin{aligned}dy(t) = &[-Cy(t) + (A + \triangle A_2(t))\bar{g}(y(t)) \\ &+ (B + \triangle B_2(t))g(y(t - \tau(t))) + I + u(t)]\,dt \\ &+ h(t, e(t), e(t - \tau(t)))d\varpi(t),\end{aligned} \tag{10}$$

where $\varpi(t)$ is a n-dimensional Brownian motion defined on the probability space $(\Omega, \mathscr{F}, P)$ with $E\{d\varpi(t)\} = 0$, $E\{d\varpi^2(t)\} = dt$, and $h(t, e(t), e(t-\tau(t))) : R^+ \times R^n \times R^n \to R^{n\times n}$ is the noise intensity which satisfies Assumption 5.

Similarly, we get the error system between systems (9) and (10) as follows:

$$\begin{aligned} de(t) = [&-Ce(t) + (A + \triangle A_2(t))f(e(t)) \\ &+ (B + \triangle B_2(t))f(e(t-\tau(t))) \\ &+ (\triangle A_2(t) - \triangle A_1(t))\bar{g}(x(t)) \\ &+ (\triangle B_2(t) - \triangle B_1(t))g(x(t-\tau(t))) \\ &+ u(t)]\,dt + h(t, e(t), e(t-\tau(t)))d\varpi(t), \end{aligned}$$

Through the above analysis, we can give the following Assumptions and Lemmas.

Assumption 1 The parameters $\triangle A_i(t)$ and $\triangle B_i(t)(i = 1, 2)$ are time-varying but norm-bounded, which satisfy

$$\begin{aligned} \triangle A_1(t) = H_1F_1(t)M_1,\ \triangle A_2(t) = H_1E_1(t)M_1, \\ \triangle B_1(t) = H_2F_2(t)M_2,\ \triangle B_2(t) = H_2E_2(t)M_2. \end{aligned}$$

where M_i and H_i $(i = 1, 2)$ are the known real constant matrices. In this paper, $M_1 = \bar{a}_{ij} - \underline{a}_{ij}$, $M_2 = \bar{b}_{ij} - \underline{b}_{ij}$ and $H_i = diag\{\frac{1}{2}, \frac{1}{2}, \ldots, \frac{1}{2}\}$, $F_i(t)$ and $E_i(t)$ are unknown real matrices with appropriate dimension and Lebesgue norm measurable elements and satisfying

$$F_i^T(t)F_i(t) \le I,\ E_i^T(t)E_i(t) \le I.$$

Assumption 2 The activation function $g(x)$ is bounded and it satisfies a Lipschitz condition

$$|g_i(\xi_1) - g_i(\xi_2)| \le l_i|\xi_1 - \xi_2|, i = 1, 2, ...n$$

for any $\xi_1, \xi_2 \in R$, where real constant $l_i > 0$ for any i and let $L = diag\{l_1, l_2, \ldots, l_n\}$.

Assumption 3 There exist unknown constants $\omega > 0$, $\nu > 0$, such that

$$\begin{aligned} \|\Delta A_2(t) - \Delta A_1(t)\| \le \omega, \\ \|\Delta B_2(t) - \Delta B_1(t)\| \le \nu. \end{aligned}$$

Remark 5 (see [33]) According to the boundedness of chaotic signals, there exist positive constants $l = \max_{1\le i\le n} l_i$ and $\|x\| \le \chi$, such that

$$\|\bar{g}(x(t))\| \le l\chi,\ \|g(x(t-\tau(t)))\| \le l\chi.$$

Assumption 4 For any two vectors $x, y \in R^n$ and a positive definite matrix $Q \in R^{n\times n}$, the following matrix inequality holds:

$$2x^Ty \le x^TQx + y^TQ^{-1}y.$$

Assumption 5 The noise matrix $h(\cdot)$ is local Lipschitz continuous and satisfies the linear growth condition as well, where $h(t, 0, 0) = 0$. Moreover, there exist two real positive matrixes Q_1, Q_2 for all x, y such that

$$trace[h^T(t, x, y)h(t, x, y)] \le x^TQ_1x + y^TQ_2y.$$

Lemma 1 *(see [27]) If X and Y are real matrices with appropriate dimensions, then there exists a number $\varepsilon > 0$, such that*

$$X^T Y + Y^T X \le \varepsilon X^T X + \frac{1}{\varepsilon} Y^T Y.$$

Lemma 2 *([28]) Assume that a continuous, positive-definite function $V(t)$ satisfies the following differential inequality:*

$$\dot{V}(t) + \alpha V^{\eta}(t) \le 0,\ \forall t \ge t_0,\ V(t_0) \ge 0,$$

where $\alpha > 0, 0 < \eta < 1$ are two constants. Then, for any given t_0, $V(t)$ satisfies the following differential inequality:

$$V^{1-\eta}(t) \le V^{1-\eta}(t_0) - \alpha(1-\eta)(t - t_0), t_0 \le t \le t_1,$$

and

$$V(t) \equiv 0, \forall t \ge t_1,$$

with t_1 given by

$$t_1 = t_0 + \frac{V^{1-\eta}(t_0)}{\alpha(1-\eta)}.$$

Lemma 3 *([29]) Let $x_1, x_2, \ldots, x_n \in R^n$ are any vectors and $0 < q < 2$ is a real number satisfying:*

$$\|x_1\|^q + \|x_2\|^q + \cdots + \|x_n\|^q \ge (\|x_1\|^2 + \|x_2\|^2 + \cdots + \|x_n\|^2)^{\frac{q}{2}}.$$

Lemma 4 *([30]) (see Wang et al., 2009): The linear matrix inequality*

$$\begin{bmatrix} Q(x) & S(x) \\ S^T(x) & R(x) \end{bmatrix} > 0,$$

where $Q(x) = Q^T(x)$, $R(x) = R^T(x)$ and $S(x)$ depend affinely on x, and it is equivalent to

$$R(x) > 0,\ Q(x) - S(x)R^{-1}(x)S^T(x) > 0.$$

Lemma 5 *([31]) Assume that the stochastic differential equation is*

$$dx(t) = f(x(t), x(t-\tau), t)dt + g(x(t), x(t-\tau), t)d\upsilon(t),$$

then an operator $\mathscr{L}V(x(t), t)$ from $R^+ \times R^n$ along the trajectory of the error system is defined as

$$\begin{aligned}\mathscr{L}V(x(t), t) &= V_t(x(t), t) + V_x(x(t), t) f(x(t), x(t-\tau), t) \\ &\quad + \frac{1}{2} trace\{g^T(x(t), x(t-\tau), t) V_{xx} g(x(t), x(t-\tau), t)\},\end{aligned}$$

where

$$\begin{aligned} V_t(x(t), t) &= \frac{\partial V(x(t), t)}{\partial t}, \\ V_x(x(t), t) &= \left(\frac{\partial V(x(t), t)}{\partial x_1}, \frac{\partial V(x(t), t)}{\partial x_2}, \ldots, \frac{\partial V(x(t), t)}{\partial x_n} \right), \\ V_{xx} &= \left(\frac{\partial^2 V(x(t), t)}{\partial x_i \partial x_j} \right)_{n \times n}. \end{aligned}$$

Remark 6 In the error systems $e(t)$ or $de(t)$, a part of the uncertainties $(\triangle A_2(t) - \triangle A_1(t))g(x(t)) + (\triangle B_2(t) - \triangle B_1(t))g(x(t-\tau(t)))$ can be as a perturbation term and design a proper controller to investigate outer synchronization based on exponent and finite-time stability theory (see reference [32]). In this paper, we use the boundedness of uncertain parameters to fill the gap for the previous researches.

3 Main Results

The controller and parameter update laws are designed as follows:

$$\begin{aligned} u(t) = & -re(t) - k_1 sign(e(t))|e(t)|^{\beta} \\ & - k_1 \frac{e_i(t)}{\|e_i(t)\|^2} \left(\int_{t-\tau(t)}^{t} e_i^T(s) e_i(s) ds \right)^{\frac{\beta+1}{2}} \\ & - l\chi \|e^T(t)\|^{-1} e(t)\hat{\omega} - l\chi \|e^T(t)\|^{-1} e(t)\hat{\nu}, \\ \dot{\hat{\omega}} = & \, l\chi \|e^T(t)\| - k_1 sign(\tilde{\omega})|\tilde{\omega}|^{\beta}, \\ \dot{\hat{\nu}} = & \, l\chi \|e^T(t)\| - k_1 sign(\tilde{\nu})|\tilde{\nu}|^{\beta}, \end{aligned} \tag{11}$$

where r is the feedback gain constant to be designed, $0 < \beta < 1$ and k_1 is a random constant. $\hat{\omega}$ and $\hat{\nu}$ are, respectively, the estimations of the bounds ω and ν, $\tilde{\omega} = \hat{\omega} - \omega$ and $\tilde{\nu} = \hat{\nu} - \nu$. And sign$(x)$ is the sign function which is defined as follows:

$$sign(x) = \begin{cases} -1, & if \ x < 0, \\ 0, & if \ x = 0, \\ 1, & if \ x > 0. \end{cases}$$

Theorem 1 *Under Assumptions 1-4, system (7) and system (8) with an impulsive effect achieve finite-time synchronization under the controller $u(t)$. If there exist a constant $r > 0$ and two positive constants θ_1 and θ_2 satisfying the following conditions:*

$$\begin{bmatrix} \Omega_0 & A & H_1 & B & H_2 \\ \star & -\frac{1}{\theta_1} I & 0 & 0 & 0 \\ \star & \star & -\frac{1}{(\theta_1 \|M_1\|^2)} & 0 & 0 \\ \star & \star & \star & -\frac{1}{\theta_2} I & 0 \\ \star & \star & \star & \star & -\frac{1}{(\theta_2 \|M_2\|^2)} \end{bmatrix} \leq 0,$$

where

$$\Omega_0 = \left(\frac{1}{1-\mu} - 2r \right) I - 2C + \frac{2}{\theta_1} L^2,$$

and

$$\begin{aligned} \frac{2}{\theta_2} L^2 - I \leq 0, \\ 0 < \tau \leq \inf_k \{t_{k+1} - t_k\}, \\ \rho_k = \max(\|I + B_k\|^2) < 1, \ k \in \ell. \end{aligned}$$

Then, synchronization is achieved in a finite time:

$$t_1 = \frac{V(0)^{1-(\beta+1)/2}}{\gamma\left(1-\frac{\beta+1}{2}\right)},$$

and

$$V(0) = e^T(0)e(0) + \frac{1}{1-\mu}\int_{-\tau(0)}^{0} e^T(s)e(s)ds + (\hat{\omega}(0)-\omega)^2 + (\hat{\upsilon}(0)-\nu)^2,$$

where $e(0)$, $\hat{\upsilon}(0)$, $\hat{\omega}(0)$ *and* $\hat{\nu}(0)$ *are the initial conditions of* e, υ, ω *and* ν, *respectively.*

We construct a Lyapunov function as follows

$$V(t) = V_1(t) + V_2(t) + V_3(t),$$

where

$$\begin{aligned} V_1(t) &= e^T(t)e(t), \\ V_2(t) &= \frac{1}{1-\mu}\int_{t-\tau(t)}^{t} e^T(s)e(s)ds, \\ V_3(t) &= \tilde{\omega}^2 + \tilde{\nu}^2. \end{aligned}$$

For $t \neq t_k$, the derivative of $V_i(t), i = 1, 2, 3$ is along the trajectories of $e(t)$. Then we have

$$\begin{aligned} \dot{V}_1(t) &= 2e^T(t)\dot{e}(t), \\ &= 2e^T(t)\left[-Ce(t) + (A+\triangle A_2(t))f(e(t)) + (B+\triangle B_2(t))f(e(t-\tau(t))) \right. \\ &\quad \left. + (\triangle A_2(t) - \triangle A_1(t))g(x(t)) + (\triangle B_2(t) - \triangle B_1(t))g(x(t-\tau(t))) + u(t)\right], \\ &= -2e^T(t)Ce(t) + 2e^T(t)(A+\triangle A_2(t))f(e(t)) + 2e^T(t)(B+\triangle B_2(t)) \\ &\quad \times f(e(t-\tau(t))) + 2e^T(t)(\triangle A_2(t) - \triangle A_1(t))g(x(t)) \\ &\quad + 2e^T(t)(\triangle B_2(t) - \triangle B_1(t))g(x(t-\tau(t))) \\ &\quad + 2e^T(t)\left[-re(t) - k_1 sign(e(t))|e(t)|^{\beta}\right. \\ &\quad - k_1\frac{e(t)}{\|e(t)\|^2}\left(\int_{t-\tau(t)}^{t} e^T(s)e(s)ds\right)^{\frac{\beta+1}{2}} \\ &\quad \left. - l\chi\|e^T(t)\|^{-1}e(t)\hat{\omega} - l\chi\|e^T(t)\|^{-1}e(t)\hat{\upsilon}\right]. \end{aligned}$$

According to Lemma 1, we get

$$\begin{aligned} 2e^T(t)(A+\triangle A_2(t))f(e(t)) &\leq \theta_1 e^T(t)AA^T e(t) + \frac{1}{\theta_1}f^T(e(t))f(e(t)) \\ &\quad + \theta_1 e^T(t)H_1E_1M_1M_1^TE_1^TH_1^Te(t) \\ &\quad + \frac{1}{\theta_1}f^T(e(t))f(e(t)), \\ &\leq e^T(t)\left[\theta_1 AA^T + \frac{2}{\theta_1}L^2 + \theta_1\|M_1\|^2H_1H_1^T\right]e(t), \end{aligned}$$

$$
\begin{aligned}
2e^T(t)(B+\triangle B_2(t))f(e(t-\tau(t))) &\le \theta_2 e^T(t)BB^Te(t)\\
&\quad+\frac{1}{\theta_2}f^T(e(t-\tau(t)))f(e(t-\tau(t)))\\
&\quad+\theta_2 e^T(t)H_2E_2M_2M_2^TE_2^TH_2^Te(t)\\
&\quad+\frac{1}{\theta_2}f^T(e(t-\tau(t)))f(e(t-\tau(t))),\\
&\le e^T(t)\left[\theta_2BB^T+\theta_2\|M_2\|^2H_2H_2^T\right]e(t)\\
&\quad+\frac{2}{\theta_2}e^T(t-\tau(t))L^2e(t-\tau(t)),
\end{aligned}
$$

It is clear from Assumptions 3,4 and Remark 5 that

$$
\begin{aligned}
&2e^T(t)(\triangle A_2(t)-\triangle A_1(t))g(x(t))\\
&\quad+2e^T(t)(\triangle B_2(t)-\triangle B_1(t))g(x(t-\tau(t)))\\
&\quad\le 2\|e^T(t)\|\omega l\chi+2\|e^T\|\nu l\chi,\\
&\quad= 2\|e^T(t)\|l\chi(\omega+\nu).
\end{aligned}
$$

Based on the above analyses, we have

$$
\begin{aligned}
\dot V_1(t) \le\ & -2e^T(t)Ce(t)+e^T(t)\left(\theta_1AA^T+\frac{2}{\theta_1}L^2+\theta_1\|M_1\|^2H_1H_1^T\right)e(t)\\
&+e^T(t)\left(\theta_2BB^T+\theta_2\|M_2\|^2H_2H_2^T\right)e(t)+\frac{2}{\theta_2}e^T(t-\tau(t))L^2e(t-\tau(t))\\
&-2l\chi\|e^T(t)\|\hat\omega-2l\chi\|e^T(t)\|\hat\nu+2\|e^T(t)\|l\chi(\omega+\nu)-2e^T(t)re(t)\\
&-2k_1|e^T(t)e(t)|^{\frac{\beta+1}{2}}-2k_1\left(\int_{t-\tau(t)}^{t}e^T(s)e(s)ds\right)^{\frac{\beta+1}{2}}.
\end{aligned}
$$

Then, the following inequalities are obtained

$$
\begin{aligned}
\dot V_2(t) &= \frac{1}{1-\mu}e^T(t)e(t)-\frac{1-\dot\tau(t)}{1-\mu}e^T(t-\tau(t))e(t-\tau(t)),\\
&\le \frac{1}{1-\mu}e^T(t)e(t)-e^T(t-\tau(t))e(t-\tau(t)),\\
\dot V_3(t) &= 2\tilde\omega\dot{\tilde\omega}+2\tilde\nu\dot{\tilde\nu},\\
&= +2(\hat\omega-\omega)l\chi\|e^T(t)\|-2k_1|\tilde\omega^2|^{\frac{\beta+1}{2}}\\
&\quad+2(\hat\nu-\nu)l\chi\|e^T(t)\|-2k_1|\tilde\nu^2|^{\frac{\beta+1}{2}}.
\end{aligned}
$$

Synthesizing the above $V_i(t)$, $i=1,2,3$, we yield

$$
\begin{aligned}
\dot V(t) &= \sum_{i=1}^{3}V_i(t),\\
&\le e^T(t)\Omega_1e(t)+e^T(t-\tau(t))\Omega_2e(t-\tau(t))-\gamma\left(|e^T(t)e(t)|^{\frac{\beta+1}{2}}\right.\\
&\quad\left.+\left(\frac{1}{1-\mu}\int_{t-\tau(t)}^{t}e^T(s)e(s)ds\right)^{\frac{\beta+1}{2}}+|\tilde\omega^2|^{\frac{\beta+1}{2}}+|\tilde\nu^2|^{\frac{\beta+1}{2}}\right),
\end{aligned}
$$

where

$$\Omega_1 = \left(\frac{1}{1-\mu} - 2r\right) I - 2C + \frac{2}{\theta_1} L^2 + \theta_1 \left(AA^T + \|M_1\|^2 H_1 H_1^T\right) + \theta_2 (BB^T + \|M_2\|^2 H_2 H_2^T),$$

$$\Omega_2 = \frac{2}{\theta_2} L^2 - I,$$

and $\gamma = min\{2k_1, 2k_1(1-\mu)^{\frac{\beta+1}{2}}\}$.

Based on the constant of Theorem 1 and Schur complement in Lemma 4, we get

$$\dot{V}(t) \leq -\gamma V^{\frac{\beta+1}{2}}(t).$$

For convenience, let $1-\eta = \frac{\beta+1}{2}$, which implies that

$$V^{1-\eta}(t) \leq V^{1-\eta}(t_{k-1}) - \gamma(1-\eta)(t-t_{k-1}), \quad t \in (t_{k-1}, t_k],\ k \in \ell. \tag{12}$$

When $t = t_k$, one obtains

$$\begin{aligned} V(t_k^+) &= e^T(t)(I+B_k)^T(I+B_k)e(t) + \frac{1}{1-\mu}\int_{t-\tau(t)}^{t} e^T(s) \\ &\quad \times (I+B_k)^T(I+B_k)e(s)ds + (\tilde{\omega})^2 + (\tilde{\nu})^2, \\ &\leq \rho_k \left[e^T(t)e(t) + \frac{1}{1-\mu}\int_{t-\tau(t)}^{t} e^T(s)e(s)ds\right] \\ &\quad + (\tilde{\omega})^2 + (\tilde{\nu})^2,\ k \in \ell, \end{aligned}$$

where $\rho_k = \max(\|I+B_k\|^2),\ k \in \ell$.

According to $\rho_k < 1$, we have

$$V(t_k^+) \leq V(t_k). \tag{13}$$

Then, using the above Equations (12) and (13) imply that

$$V^{1-\eta}(t) \leq V^{1-\eta}(t_0^+) - \gamma(1-\eta)(t-t_0).$$

Proof Using Equation (12), for $k = 1$ and any $t \in (t_0, t_1]$, it is easy to obtain

$$V^{1-\eta}(t) \leq V^{1-\eta}(t_0^+) - \gamma(1-\eta)(t-t_0).$$

and the corresponding inequality is obtained

$$V^{1-\eta}(t_1) \leq V^{1-\eta}(t_0^+) - \gamma(1-\eta)(t_1-t_0).$$

From Equation (13), we also yield that

$$\begin{aligned} V^{1-\eta}(t_1^+) &\leq V^{1-\eta}(t_1), \\ &\leq V^{1-\eta}(t_0^+) - \gamma(1-\eta)(t_1-t_0). \end{aligned}$$

Similarly, for $k = 2$ and $t \in (t_1, t_2]$, one has

$$\begin{aligned} V^{1-\eta}(t) &\leq V^{1-\eta}(t_1^+) - \gamma(1-\eta)(t-t_1), \\ &\leq V^{1-\eta}(t_0^+) - \gamma(1-\eta)(t_1-t_0) \\ &\quad - \gamma(1-\eta)(t-t_1), \\ &= V^{1-\eta}(t_0^+) - \gamma(1-\eta)(t-t_0). \end{aligned}$$

In general, for $k = m + 1$ and $t \in (t_m, t_{m+1}]$, we have

$$\begin{aligned}
V^{1-\eta}(t) &\leq V^{1-\eta}(t_m^+) - \gamma\,(1-\eta)\,(t - t_m),\\
&\leq V^{1-\eta}(t_{m-1}^+) - \gamma\,(1-\eta)\,(t_m - t_{m-1})\\
&\quad -\gamma\,(1-\eta)\,(t - t_m),\\
&= V^{1-\eta}(t_{m-1}^+) - \gamma\,(1-\eta)\,(t - t_{m-1}),\\
&\leq V^{1-\eta}(t_{m-2}^+) - \gamma\,(1-\eta)\,(t_{m-1} - t_{m-2})\\
&\quad -\gamma\,(1-\eta)\,(t - t_{m-1})\},\\
&= V^{1-\eta}\left(t_{m-2}^+\right) - \gamma\,(1-\eta)\,(t - t_{m-2}),\\
&\qquad\qquad \vdots\\
&\leq V^{1-\eta}\left(t_0^+\right) - \gamma\,(1-\eta)\,(t_1 - t_0)\\
&\quad -\gamma\,(1-\eta)\,(t - t_0)\},\\
&= V^{1-\eta}\left(t_0^+\right) - \gamma\,(1-\eta)\,(t - t_0).
\end{aligned}$$

Then, we obtain

$$V^{1-\eta}(t) \leq V^{1-\eta}(t_0^+) - \gamma(1-\eta)(t - t_0).$$

Therefore, from Lemma 1, the finite-time robust synchronization is obtained for MNN with impulsive effect, and the finite-time is given as:

$$t_1 = \frac{V(0)^{1-(\beta+1)/2}}{\gamma\left(1 - \frac{\beta+1}{2}\right)}.$$

The proof is completed.

Next, we consider the robust synchronization of MNN under stochastic perturbation. □

Theorem 2 *Under Assumptions 1-5, the system (10) with stochastic perturbations will converge under the same controller $u(t)$ as in Theorem 1. If there exist a constant $r > 0$, and two positive constants θ_1 and θ_2 which satisfy some certain conditions, then systems (9) and (10) achieve finite-time synchronization. Hence, the following conditions hold:*

$$\begin{bmatrix}
\Omega_1 & A & H_2 & B & H_3\\
\star & -\frac{1}{\theta_1}I & 0 & 0 & 0\\
\star & \star & -\frac{1}{(\theta_1\|M_1\|^2)} & 0 & 0\\
\star & \star & \star & -\frac{1}{\theta_2}I & 0\\
\star & \star & \star & \star & -\frac{1}{(\theta_2\|M_2\|^2)}
\end{bmatrix} \leq 0,$$

$$\frac{2}{\theta_2}L^2 + Q_2 - I \leq 0,$$

where

$$\Omega_1 = \left(\frac{1}{1-\mu} - 2r\right)I - 2C + Q_1 + \frac{2}{\theta_1}L^2.$$

Then the drive system (9) and the response system (10) can be finite-time synchronized in mean square, and the finite time is obtained

$$t_2 = \frac{V(0)^{1-(\beta+1)/2}}{\gamma\left(1 - \frac{\beta+1}{2}\right)},$$

where the value of $V(0)$ is the same as that in Theorem 1.

A Lyapunov function is given as follows:

$$V(t) = e^T(t)e(t) + \frac{1}{1-\mu}\int_{t-\tau(t)}^{t} e^T(s)e(s)ds + \tilde{\omega}^2 + \tilde{\nu}^2.$$

From Lemma 5, we obtain the operator $\mathscr{L}V(t)$

$$\begin{aligned}\mathscr{L}V(t) = {} & 2e^T(t)\left[-Ce(t) + (A + \triangle A_2(t))f(e(t))\right.\\ & + (B + \triangle B_2(t))f(e(t-\tau(t))) + (\triangle A_2(t) - \triangle A_1(t))g(x(t))\\ & \left. + (\triangle B_2(t) - \triangle B_1(t))g(x(t-\tau(t))) + u(t)\right]\\ & + trace\left[h^T(t, e(t), e(t-\tau(t)))h(t, e(t), e(t-\tau(t)))\right]\\ & + \frac{1}{1-\mu}e^T(t)e(t) - \frac{1-\dot{\tau}(t)}{1-\mu}e^T(t-\tau(t))e(t-\tau(t))\\ & + 2\tilde{\omega}\dot{\tilde{\omega}} + 2\tilde{\nu}\dot{\tilde{\nu}}.\end{aligned}$$

From Assumption 5, we have

$$\begin{aligned}& trace[h^T(t, e(t), e(t-\tau(t)))h(t, e(t), e(t-\tau(t)))\\ & \quad \le e^T(t)Q_1e(t) + e^T(t-\tau(t))Q_2e(t-\tau(t)).\end{aligned}$$

According to the proof of Theorem 1, we get

$$\begin{aligned}\mathscr{L}V(t) \le {} & e^T(t)\Omega_3e(t) + e^T(t-\tau(t)\Omega_4e(t-\tau(t)) - \gamma\left(|e^T(t)e(t)|^{\frac{\beta+1}{2}}\right.\\ & \left. + \left(\frac{1}{1-\mu}\int_{t-\tau(t)}^{t} e^T(s)e(s)ds\right)^{\frac{\beta+1}{2}} + |\tilde{\omega}^2|^{\frac{\beta+1}{2}} + |\tilde{\nu}^2|^{\frac{\beta+1}{2}}\right),\end{aligned}$$

where

$$\begin{aligned}\Omega_3 = {} & \left(\frac{1}{1-\mu} - 2r\right)I - 2C + Q_1 + \frac{2}{\theta_1}L^2\\ & + \theta_1\left(AA^T + \|M_1\|^2H_1H_1^T\right) + \theta_2\left(BB^T + \|M_2\|^2H_2H_2^T\right),\\ \Omega_4 = {} & \frac{2}{\theta_2}L^2 + Q_2 - I,\end{aligned}$$

and $\gamma = min\{2k_1, 2k_1(1-\mu)^{\frac{\beta+1}{2}}\}$.

With the condition of Theorem 2, we get

$$\mathscr{L}V(t) \le -\gamma V^{\frac{\beta+1}{2}}(t).$$

Taking the expectation on both sides of the above equation, it can be written

$$E[\mathscr{L}V(t)] \le -\gamma E[V^{\frac{\beta+1}{2}}(t)].$$

For any $t_0 \ge \tau > 0$*, we can easily obtain*

$$E[V^{\frac{\beta+1}{2}}(t_0)] = (E[V(t_0)])^{\frac{\beta+1}{2}}.$$

Therefore, we yield

$$E[\mathscr{L}V(t)] \le -\gamma(E[V(t)])^{\frac{\beta+1}{2}}.$$

According to the finite-time stabilization theory of Lemma 2, $E[V(t)]$ converges to zero in a finite time t_2, and t_2 is estimated by

$$t_2 = \frac{V(0)^{1-(\beta+1)/2}}{\gamma\left(1-\frac{\beta+1}{2}\right)}.$$

The proof is completed.

Remark 7 Comparing with other memristive neural network [3,4,7,11], the synchronization performance is investigated based on a new analysis approach instead of using differential inclusions theory and set-valued mappings technique, which may be less conservative than synchronization criterion obtained by using existing methods. Especially, we deal with the issue of parameter mismatch in process of the memristive neural network.

Remark 8 In this paper, we combine the analysis method of traditional neural network [20,21,30] and overcome the issue of parameter mismatch to investigate memristive neural network [19], which is more practical significance to explore the biological neural network.

4 Numerical Examples

In this section, two numerical examples are given to demonstrate the effectiveness of our proposed scheme.

Consider a MNN system with time-varying delays as follows:

$$\begin{aligned}\dot{x}_i(t) = -c_i x_i(t) + \sum_{j=1}^{2} a_{ij}(x_i(t))g_j(x_j(t)) \\ + \sum_{j=1}^{2} b_{ij}(x_i(t))g_j(x_j(t-\tau(t))) + I_i,\end{aligned} \tag{14}$$

where $i = 1, 2$, $I_1 = I_2 = 0$, $g_i(x_i(t)) = tanh(x_i)$, $\tau(t) = 0.2cost$, which means that $\tau = 0.2$ and $\mu = 0.2$ and $c_1 = 1, c_2 = 1.5$. The remaining parameters are given with (15)-(18) and

$$a_{11}(x_1) = \begin{cases} 0.7, & |x_1(t)| \le 1, \\ 0.3, & |x_1(t)| > 1, \end{cases} \quad a_{12}(x_1) = \begin{cases} 1.5, & |x_1(t)| \le 1, \\ 0.5, & |x_1(t)| > 1, \end{cases} \tag{15}$$

$$a_{21}(x_2) = \begin{cases} -0.1, & |x_2(t)| \le 1, \\ -0.3, & |x_2(t)| > 1, \end{cases} \quad a_{22}(x_2) = \begin{cases} 0.1, & |x_2(t)| \le 1, \\ 0.9, & |x_2(t)| > 1. \end{cases} \tag{16}$$

$$b_{11}(x_1) = \begin{cases} -1.5, & |x_1(t)| \le 1, \\ -1.3, & |x_1(t)| > 1, \end{cases} \quad b_{12}(x_1) = \begin{cases} -0.1, & |x_1(t)| \le 1, \\ -0.05, & |x_1(t)| > 1, \end{cases} \tag{17}$$

$$b_{21}(x_2) = \begin{cases} -0.15, & |x_2(t)| \le 1, \\ -0.2, & |x_2(t)| > 1, \end{cases} \quad b_{22}(x_2) = \begin{cases} -2.3, & |x_2(t)| \le 1, \\ -2.5, & |x_2(t)| > 1. \end{cases} \tag{18}$$

Then, we obtain (19)-(21) as follows:

$$A = \begin{pmatrix} 0.5 & 1 \\ -0.2 & 0.5 \end{pmatrix}, \quad \tilde{A} = \begin{pmatrix} 0.2 & 0.5 \\ 0.1 & 0.4 \end{pmatrix}, \quad M_1 = \begin{pmatrix} 0.4 & 1 \\ 0.2 & 0.8 \end{pmatrix}, \tag{19}$$

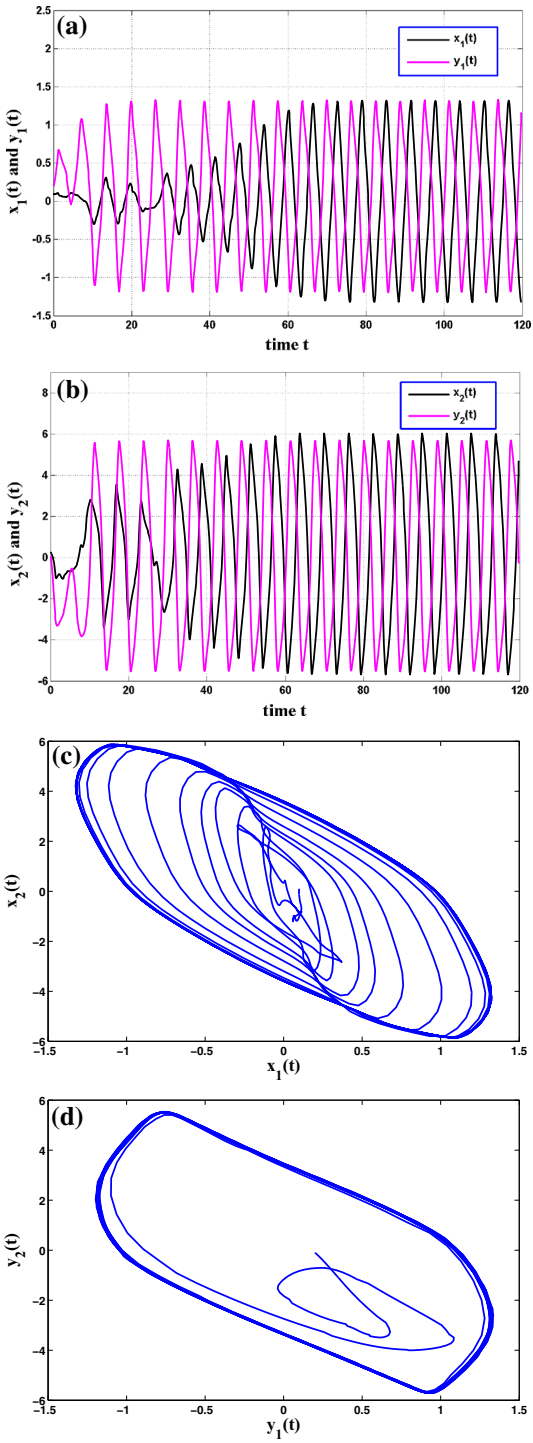

Fig. 6 **a** and **b** are time response curves of state variables without the controller $u(t)$, **c** and **d** are the phase curves of systems (14) and (22) without the controller $u(t)$

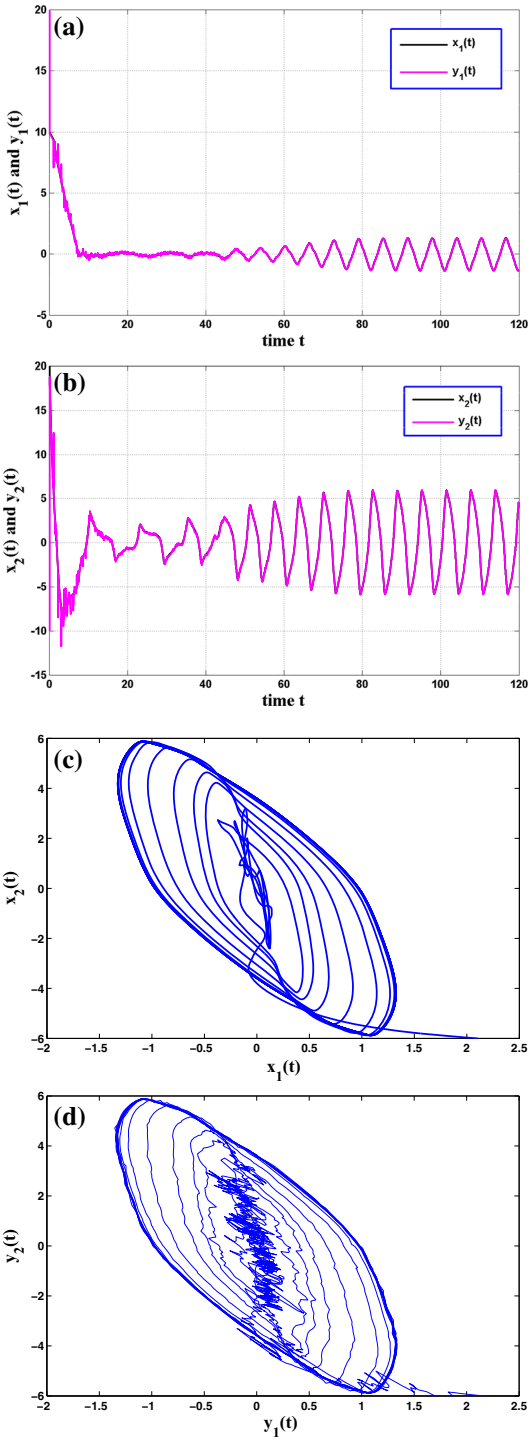

Fig. 7 **a** and **b** are time response curves of state variables with the controller $u(t)$, **c** and **d** are the phase curves of systems (14) and (22) with the controller $u(t)$

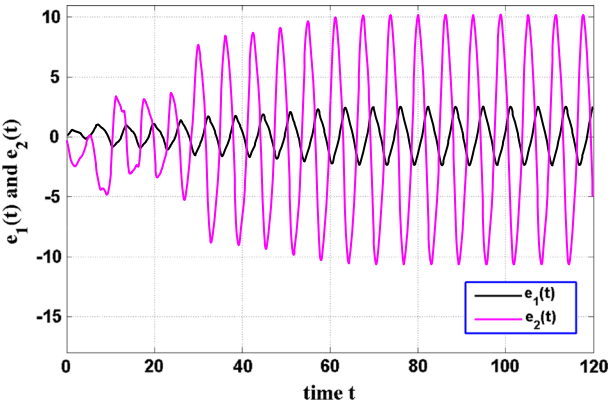

Fig. 8 (Color online) The synchronization errors e_1, e_2 of systems (14) and (22) without the controller $u(t)$

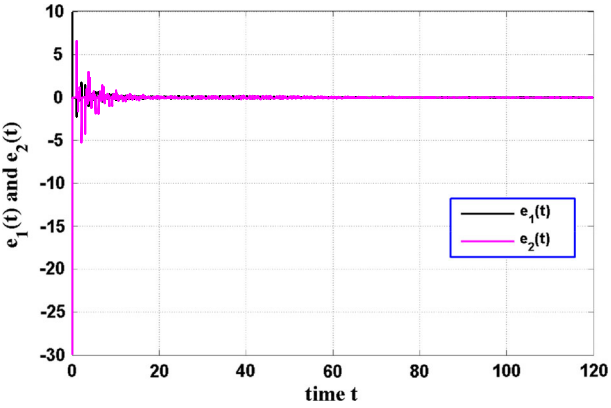

Fig. 9 (Color online) The synchronization errors e_1, e_2 of systems (14) and (22) with the controller $u(t)$

$$B = \begin{pmatrix} -1.4 & -0.175 \\ -0.075 & -2.4 \end{pmatrix}, \quad \tilde{B} = \begin{pmatrix} 0.1 & 0.025 \\ 0.025 & 0.1 \end{pmatrix}, \tag{20}$$

$$M_2 = \begin{pmatrix} 0.2 & 0.05 \\ 0.05 & 0.2 \end{pmatrix}, \; H_1 = H_2 = \begin{pmatrix} 0.5 & 0 \\ 0 & 0.5 \end{pmatrix}, \; L = \begin{pmatrix} 1 & 0 \\ 0 & 1 \end{pmatrix}, \tag{21}$$

and $F_i(t) \in [-1, 1]$, $i = 1, 2$.

Example 1 System (14) as the drive system is given, and the corresponding response system with impulsive effect is considered as follows:

$$\begin{aligned} \dot{y}_i(t) = &-c_i y_i(t) + \sum_{j=1}^{2} a_{ij}\left(y_i(t)\right) g_j\left(y_j(t)\right) + \sum_{j=1}^{2} b_{ij}\left(y_i(t)\right) \\ &\times g_j(y_j\left(t - \tau(t)\right)) + I_i + u_i(t), \; t \neq t_k, \\ \triangle y_i(t) = &\, y_i(t_k^+) - y_i(t_k^-) = B_{ik} e_i, \; t = t_k, \; k \in \ell, \end{aligned} \tag{22}$$

where $B_{ik} = -0.2$.

Let $r = 100$, according to the LMI toolbox, we obtain $\theta_1 = 101.0101$, $\theta_2 = 3.006$. We choose $l = 1$, $\chi = 1.6$, $x(0) = (10, 20)^T$ and $y(0) = (20, -10)^T$. Figures 6, 7 show the

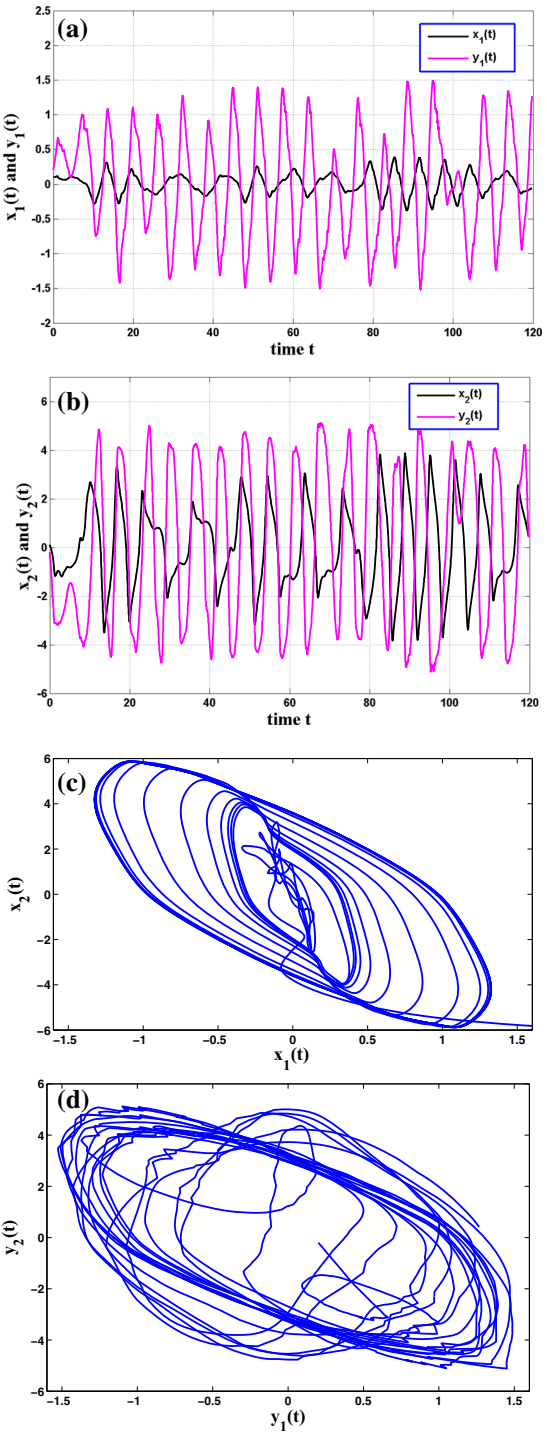

Fig. 10 **a** and **b** are time response curves of state variables without the controller $u(t)$, **c** and **d** are the phase curves of systems (14) and (23) without the controller $u(t)$

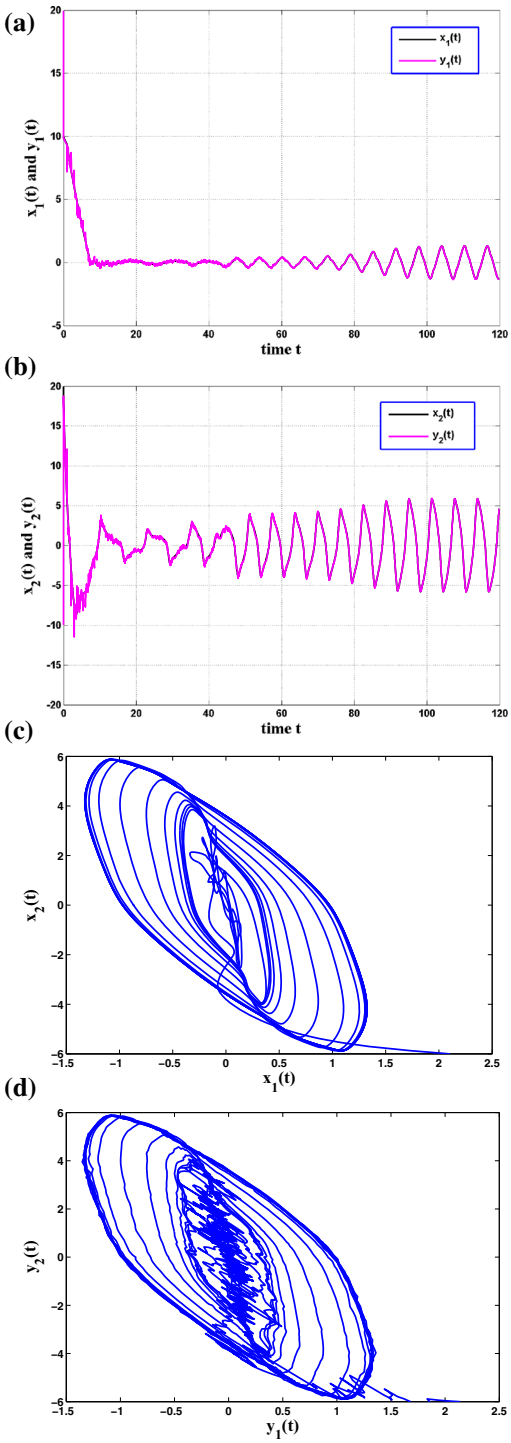

Fig. 11 **a** and **b** are time response curves of state variables with the controller $u(t)$, **c** and **d** are the phase curves of systems (14) and (23) with the controller $u(t)$

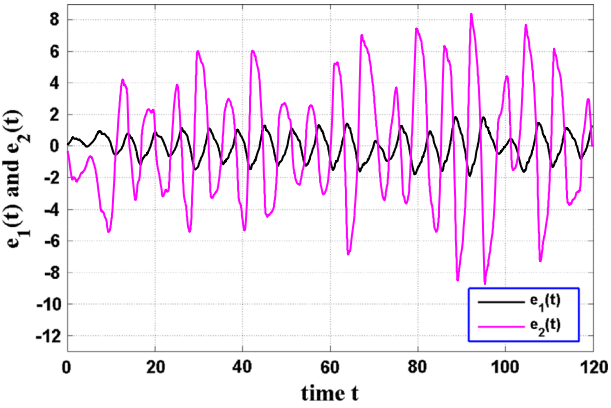

Fig. 12 (Color online) The synchronization errors e_1, e_2 of systems (14) and (23) without the controller $u(t)$

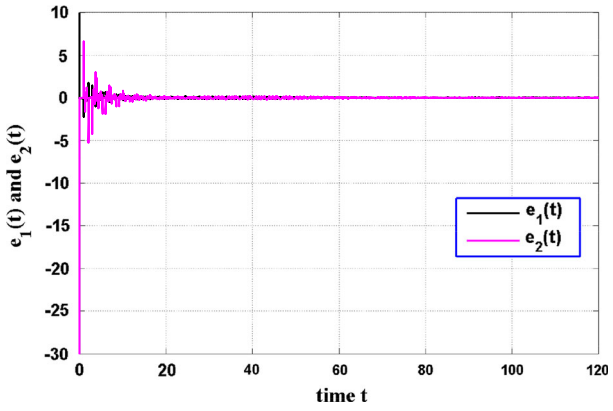

Fig. 13 (Color online) The synchronization errors e_1, e_2 of systems (14) and (23) with the controller $u(t)$

time response of the state variables and the phase plots of the drive-response system (14) and (22) without and with the controller $u(t)$. Figures 8, 9 give the corresponding error curves without and with the controller $u(t)$ designed in (22).

Example 2 System (14) as the drive system is given and the corresponding response system with stochastic perturbation is considered as follows:

$$\begin{aligned} dy_i(t) = &\Bigg[-c_i y_i(t) + \sum_{j=1}^{2} a_{ij}(y_i(t)) g_j(y_j(t)) \\ &+ \sum_{j=1}^{2} b_{ij}(y_i(t)) g_j(y_j(t-\tau(t))) + I_i + u_i(t) \Bigg] dt \\ &+ h(t, e(t), e(t-\tau(t)))d\varpi(t), \end{aligned} \tag{23}$$

where the noise intensity is given as follows:

$$\begin{cases} h_1(t, e_1(t), e_1(t-\tau(t))) = \sqrt{0.005}e_1(t) + \sqrt{0.25}e_1(t-\tau(t)), \\ h_2(t, e_2(t), e_2(t-\tau(t))) = \sqrt{0.025}e_2(t) + \sqrt{0.005}e_2(t-\tau(t)). \end{cases}$$

where $h(t, e(t), e(t-\tau(t))) = diag(h_1(t, e_1(t), e_1(t-\tau(t))), h_2(t, e_2(t), e_2(t-\tau(t)))$ $\varpi(t) = (\varpi_1(t), \varpi_2(t))^T$ is a 2-dimensional Brownian motion satisfying $E\{d\varpi(t)\} = 0$ and $E\{[d\varpi(t)]^2\} = dt$. From Assumption 3, it is easy to get $Q_1 = diag(0.01, 0.05)$, $Q_2 = diag(0.5, 0.01)$. The remaining parameters are the same as in Example 1. Figures 10, 11 show the time response of the state variables and the phase plots of the drive-response system (14) and (23) without and with the controller $u(t)$. Figures 12, 13 give the corresponding error curves without and with the controller $u(t)$ designed in (23).

5 Conclusion and Prospect

In this paper, based on both the impulsive analytical technique and the performance of stochastic differential equation, finite-time synchronization of a MNN with impulsive effect and stochastic perturbation have been studied. Especially, different from previous analysis technique, our research use a novel transformation way which transforms the MNN into cNN with uncertain parameters to study finite-time synchronization of MNN based on the drive-response concept and the finite-time stability theory. Our results on the dynamical behaviour of MNN extend and improve some existing ones. Numerical simulations verify the effectiveness of our theoretical analysis.

Following the research of the MNN, it is necessary to further attempt and explore real models and dynamic behavior of MNN, which provide an in-depth understanding of key design implications of memristor-based memories. Previous research has shown that the MNN is a more realistic model for the description of real neural systems, so it is very interesting to investigate the MNN. However, few researchers focussed on the in-depth analysis in the model of MNN and the corresponding memory performance of the memristor.

Acknowledgements The authors thank all the Editor and the anonymous referees for their constructive comments and valuable suggestions, which are helpful to improve the quality of this paper. The work is supported by the National Key Research and Development Program (Grant Nos. 2016YFB0800602, 2016YFB0800604) and the National Natural Science Foundation of China (Grant Nos. 61472045, 61573067).

References

1. Chua LO (1971) Memristorthe missing circuit element. IEEE Trans Circuit Theory 18:507–519
2. Thomas A (2013) Memristor-based neural networks. J Phys D: Appl Phys 46:093001–0930012
3. Chen L, Wu R, Cao J, Liu J (2015) Stability and synchronization of memristor-based fractional-order delayed neural networks. Neural Netw 71:37–44
4. Abdurahman A, Jiang H, Teng Z (2015) Finite-time synchronization for memristor-based neural networks with time-varying delays. Neural Netw 69:20–28
5. Zhang G, Hu J, Shen Y (2015) New results on synchronization control of delayed memristive neural networks. Nonlinear Dynamic 81:1167–1178
6. Luo Y, Sun Q, Zhan H, Cui L (2015) Adaptive critic design-based robust neural network control for nonlinear distributed parameter systems with unknown dynamics. Neurocomputing 148:200–208
7. Zhao H, Li L, Peng H, Kurths J, Xiao J, Yang Y (2015) Anti-synchronization for stochastic memristor-based neural networks with non-modeled dynamics via adaptive control approach. Eur Phys J B 88:1–10
8. Zhao H, Li L, Peng H, Xiao J, Yang Y (2015) Mean square modified function projective synchronization of uncertain complex network with multi-links and stochastic perturbations. Eur Phys J B 88:1–8
9. Bao H, Cao J (2015) Projective synchronization of fractional-order memristor-based neural networks. Neural Netw 63:1–9
10. Ding S, Wang Z (2015) Stochastic exponential synchronization control of memristive neural networks with multiple time-varying delays. Neurocomputing 162(2015):16–25

11. Song Y, Wen S (2015) Synchronization control of stochastic memristor-based neural networks with mixed delays. Neurocomputing 156:121–128
12. Duan S, Hu X, Dong Z, Wang L, Mazumder P (2015) Memristor-based cellular nonlinear/neural network: design. Analysis, and applications. IEEE Trans Neural Netw Learn Syst 26:1202–1213
13. Wu H, Zhang L (2013) Almost periodic solution for memristive neural networks with time-varying delays. J Appl Math 716172:1–12
14. Li L, Ho DWC, Cao J, Lu J (2016) Pinning cluster synchronization in an array of coupled neural networks under event-based mechanism. Neural Netw 76:1–12
15. Wen S, Zeng Z, Huang T (2012) Adaptive synchronization of memristor-based Chua's circuits. Phys Lett A 376:2775–2780
16. Zhao H, Li L, Peng H, Xiao J, Yang Y, Zheng M (2016) Impulsive control for synchronization and parameters identification of uncertain multi-links complex network. Nonlinear Dynamic 83:1437–1451
17. Mathiyalagan K, Parka JH, Sakthivel R (2015) Synchronization for delayed memristive BAM neural networks using impulsive control with random nonlinearities. Appl Math Comput 259:967–979
18. Zhang G, Shen Y (2015) Exponential stabilization of memristor-based Chaotic neural networks with time-varying delays via intermittent control. IEEE Trans Neural Netw Learn Syst 26:1431–1441
19. Zhao H, Li L, Peng H, Xiao J, Yang Y (2016) Finite-time boundedness analysis of memristive neural network with time-varying delay. Neural Process Lett. doi:10.1007/s11063-015-9487-5
20. Liu B, Liu X, Chen G, Wang H (2005) Robust impulsive synchronization of uncertain dynamical networks. IEEE Trans Circuits Syst-I: Regul Pap 52:1901–1906
21. Fang Y, Yan K, Li K (2014) Robust adaptive exponential synchronization of stochastic perturbed chaotic delayed neural networks with parametric uncertainties. Math Probl Eng 963081:1–12
22. Lu J, Wang Z, Cao J, HO DWC, Kurths J (2012) Pinning impulsive stabilization of nonlinear dynamical networks with time-delay. Int J Bifurc Chaos 22:1250176-1–1250176-12
23. Lu J, Ding C, Lou J, Cao J (2015) Outer synchronization of partially coupled dynamical networks via pinning impulsive controllers. J Franklin Inst 352:5024–5041
24. Dorato P (1961) Short-time stability in linear time-varying system. Proc IRE Int Conv Rec Part 4:83–87
25. Guo Z, Wang J, Yan Z (2014) Attractivity analysis of Memristor-based cellular neural networks with time-varying delays. IEEE Trans Neural Netw Learn Syst 25:704–717
26. Li L, Ho DWC, Lu J (2013) A unified approach to practical consensus with quantized data and time delay. IEEE Trans Circuits Syst 60:2668–2678
27. Boyd S, Ghaoui LE, Feron E, Balakrishnan V (1994) Linear matrix inequalities in system and control theory. SIAM, Philadelphia
28. Tang Y (1998) Terminal sliding mode control for rigid robots. Automatica 34:51–56
29. Mei J, Jiang M, Wang B, Long B (2013) Finite-time parameter identification and adaptive synchronization between two chaotic neural networks. J Franklin Inst 350:1617–1633
30. Wang J, Jian J, Yan P (2009) Finite-time boundedness analysis of a class of neutral type neural networks with time delays. ISNN 2009 5551:395–404.
31. Mao X (2002) A note on the LaSalle-type theorems for stochastic differential delay equations. J Math Anal Appl 268:125–142
32. Yang X, Ho DWC (2015) Synchronization of delayed memristive neural networks: robust analysis approach. IEEE Trans Cybern. doi:10.1109/TCYB.2015.2505903
33. Zhang H, Ma T, Huang GB et al (2010) Robust global exponential synchronization of uncertain chaotic delayed neural networks via dual-stage impulsive control. IEEE Trans Syst Man Cybern Part B Cybern A Publ IEEE Syst Man and Cybern Soc 40(3):831–844